The 4th European sCO_2 Conference for Energy Systems
March 23-24, 2021, Online Conference

2021-sCO2.eu-107

NUMERICAL INVESTIGATION OF A SIMPLE REGENERATIVE HEAT TO POWER SYSTEM WITH COUPLED OR INDEPENDENT TURBOMACHINERY DRIVES

Matteo Marchionni*
Brunel University London
Uxbridge, United Kingdom
Email:matteo.marchionni@brunel.ac.uk

Giuseppe Bianchi
Brunel University London
Uxbridge, United Kingdom

Muhammad Usman
Brunel University London
Uxbridge, United Kingdom

Apostolos Pesyridis
Brunel University London
Uxbridge, United Kingdom

Savvas A. Tassou
Brunel University London
Uxbridge, United Kingdom

ABSTRACT

Supercritical CO_2 (sCO_2) power systems have the potential to revolutionise power generation. Among the possible layouts, the simple regenerative cycle is the most essential, yet potentially the most competitive for an industrial uptake of the sCO_2 technology at small-scales (<0.5MW_e) in high-grade waste heat to power applications (>400°C). To compensate for the efficiency downsides due to the basic architecture, this study investigates how turbomachinery could improve the design and part-load performance of sCO_2 power systems. With reference to the 50kW_e High Temperature Heat To power Conversion facility (HT2C) available at Brunel University London, this research numerically assesses pros and cons of a radial turbine and a compressor being simultaneously or independently driven. Two turbine designs with nominal total-static efficiency of 75% were developed using a mean-line methodology which further allowed to retrieve the operational and efficiency maps. These maps were later implemented in a one-dimensional simulation platform of the HT2C facility calibrated against equipment data. The differential performance of the coupled and independent turbomachinery drive solutions was assessed with reference to a broad range of industrial heat input conditions in terms of mass flow rate and temperature of the flue gas. The results show marginal benefits at design conditions due to the same turbine design specifics. The independent drive solution leads to worse performance for part load conditions below the nominal one. On the other hand, the dual optimisation of compressor and turbine speeds allows substantial benefits above the design point, particularly for deviations of the flue gas temperature. At 110% of the nominal heat source temperature, the independent drive solution increases the net thermal power output by 27%, namely from 75kW to 95kW. This is primarily due to a higher mass flow rate in the sCO_2 loop as well as a slightly higher pressure ratio.

INTRODUCTION

Supercritical CO_2 power has been receiving a large interest from the academic and industrial communities in the last decade [1]. The use of direct Joule-Brayton cycles in which the compression process takes place in the critical region indeed allows to increase the net power output with respect to a compression of CO_2 in the gas state [2]. Furthermore, the use of CO_2 as working fluid allows to overcome the temperature limitation of steam cycles, even the state-of-the-art ones [3]. Lastly yet importantly, the use of a high-pressure, non-toxic and non-flammable working fluid provides benefits in terms of footprint, safety as well as operational flexibility. This is a key requirement for thermal power generation during the next decades [4]. In fact, baseload power stations will be asked to adapt their load not only depending on the electricity demand but also based on the increasing penetration of renewable sources in the energy mix [5]. Despite these advantages, the Technology Readiness Level (TRL) of sCO_2 power equipment is still not sufficiently mature for a mass deployment, even though there are already commercial solutions up to 8 MW_e [6] and large pilot test facilities up to 10 MW_e (STEP) [7], 50MW_{th} (Net Zero) [8] or 300 MW_e (Allam Cycle Zero Emission Coal Power) [9] which are currently at a more advanced TRL.

A key shortcoming that sCO_2 power technology is currently experiencing is the large capital expenditure in comparison with Steam or Organic Rankine Cycles. Even though plenty of studies have been published on cycle analysis [10], optimal layouts seem to be the streamlined ones, such the simple regenerative [11] or recompressed cycles [12]. In the available experimental facilities based on the afore mentioned architectures, the turbomachines are of radial type due to the low pressure ratio and small mass flow rate [13]. More specifically, mature layouts consider the use

* corresponding author(s)

DOI: 10.17185/duepublico/73949

of a power turbine directly coupled with the electric generator and an ancillary pump [6, 14] or turboalternator [15] to provide flow to the CO_2 loop. Other test facilities instead employ a single shaft turbomachinery layout which constraints turbine and compressor to rotate at the same speed [16]. If on one hand independent drives of pump/compressor may lead to better performance, a single turbomachinery drive is definitely more cost effective. This is true especially for small-scale sCO_2 power units (<0.5MWe), such as the ones for high-grade waste to power conversion that find potential applications in the iron and steel, cement, and glass industries [17].

From a scientific viewpoint, there is a lack of complex cycle optimisation studies since this kind of investigations require detailed equipment models that eventually need to be linked together at system level. As concerns the turbomachinery modelling, this implies retrieving the maps from test data [18] or numerical mean line [19] or 3D CFD [4] simulations. An alternative approach to operating maps is the use of non-dimensional curves based on load and flow coefficients [20]. With regards to heat exchangers, off-design modelling approaches based on the global heat transfer coefficient have been developed [21]. However, such formulations are not optimal for dynamic and control studies given their less accurate predictions during transient operations and when the thermophysical properties show a high variability with the CO_2 temperature and pressure. Therefore, one dimensional models become a suitable trade-off between computational cost and accuracy.

In this paper, we investigated the performance impact of independent and coupled turbomachinery layouts for a small-scale heat to power system based on the High Temperature Heat To power Conversion facility (HT2C) available at Brunel University London [16]. This sCO_2 rig is based on a simple regenerative cycle and has 50 kWe as nominal power output. Strengths and novel features of this study are the development of a numerical simulation platform calibrated on actual equipment data and the use of an innovative design methodology [22] to retrieve the turbomachinery operating maps. The comparison is made with reference to the same compressor and two turbine design configurations for each drive case.

SYSTEM DESCRIPTION

An overview of the HT2C facility is shown in Figure 1.a. The modelled sCO_2 system, displayed in Figure 1, employs three heat exchangers, two radial machines mounted on the same shaft, a receiver to prevent the fluid thermal expansion during transients and a series of valves, pipes and ancillaries. The standard 20ft container (Figure 1.b) gathers all the system components of the sCO_2 packaged unit except for the waste heat recovery unit, i.e. the primary heater of the sCO_2 loop, which is located along the exhaust line of the Process Air Heater (Figure 1.a). The primary heater and the sCO_2 loop are connected through two 10-meter pipes.

The direct heat recovery from the waste source is performed in the primary heater, where the adopted micro-tube technology allows to enhance the heat transfer between the flue gas (shell side) and the CO_2 (tube side) without an excessive pressure drop on the gas side. A Printed Circuit Heat Exchanger (PCHE) and a Plate Heat Exchanger (PHE) are used as recuperator and gas cooler respectively.

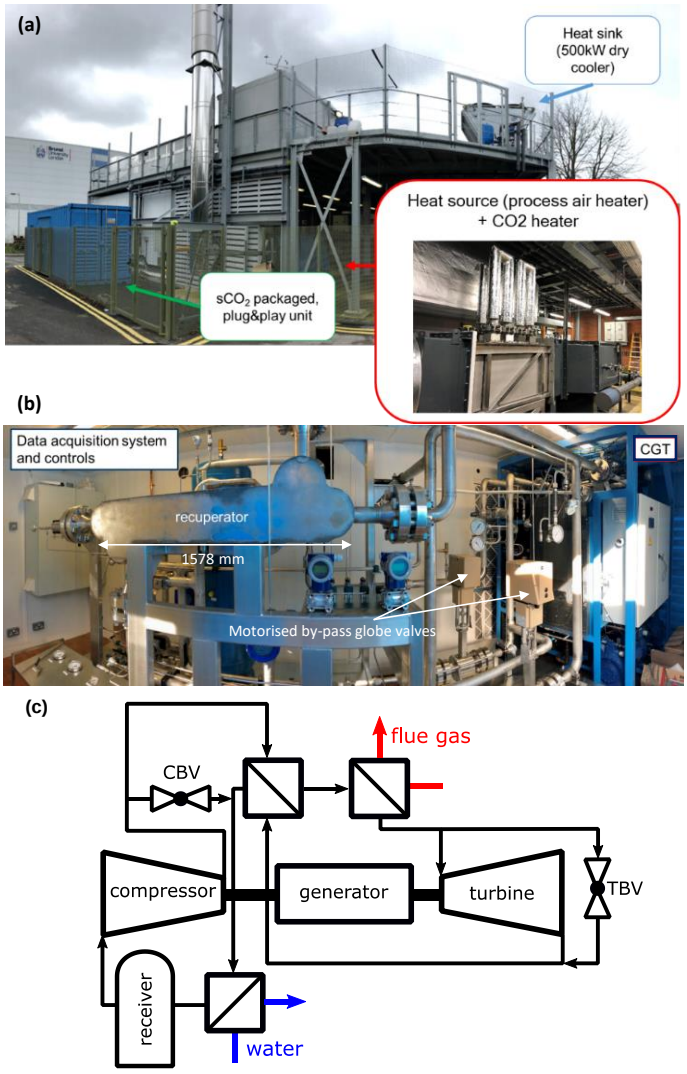

Figure 1: High Temperature Heat To power Conversion facility (HT2C) at Brunel University London: facility overview (a), sCO_2 loop inside the blue container shown in (b) and system layout (c).

In the Compressor-Generator-Turbine (CGT) assembly, which can be also seen on the right-hand side of Figure 1.b, the heat to power conversion occurs. A radial compressor and a turbine are mounted on the same shaft of a synchronous brushless generator. A complex ancillary system is used to ensure lubrication of the bearings and to reduce windage losses [23]. Two motorised compressor and turbine by-pass globe valves, shown in Figure 1.b, have been foreseen to control the system at nominal, startup, shutdown and emergency operations.

The waste heat source is simulated by a Process Air Heater, able to provide a flow of exhaust gases up to 1 kg/s at 1073.15K.

The heat sink is instead a 500 kW dry cooler system. The dry-cooler rejects the heat from a water/glycol mixture which, in turn, removes the residual heat from the CO_2 in the PHE gas cooler. Variable speed drives for the water pump and fans allow the variation of the heat removal and rejection rate.

A data acquisition system has been also installed in the container (left-hand side of Figure1.b) to allow the remote control and monitoring of the unit. A thorough description of the HT2C facility is reported in [16].

MODELLING METHODOLOGY

The model of the sCO_2 heat to power conversion system has been developed in the commercial software GT-SUITE™, a CAE simulation platform based on a one-dimensional (1D) formulation of Navier-Stokes equations and on a staggered grid spatial discretization. This software tool allows to model each component independently through accurate input data, which relate to the geometrical features of the components as well as their performance data. This information can result either from an experimental campaign or, as in the current case, from more detailed or complex models. Each component can then be considered as a lumped or an equivalent 1D object. In the latter case, the object is discretized in a series of capacities, or volumes, connected by boundaries. The scalar variables (pressure, temperature, density, internal energy, enthalpy, etc.) are assumed to be uniform in each volume. On the other hand, vector variables (mass flux, velocity, mass fraction fluxes, etc.) are calculated for each boundary. The continuity, momentum and energy equations are used to calculate the mass flow rates, the pressure dynamics and the energy transfer through the volumes. The energy equation is expressed in terms of total enthalpy and its solution requires the computation of the local heat transfer coefficient through calibrated heat transfer correlations. A more detailed description of the modelling methodology is provided in [19, 24].

The model block diagram of the sCO_2 system investigated in this work is reported in Figure 2. Components are denoted with uppercase letters while the boundary conditions required for the simulations are indicated with lowercase ones. These boundary conditions are the revolution speed of the compressor-generator-turbine unit as well as the inlet temperatures, pressures and mass flow rates of the hot and cold sources. In the case of coupled turbomachinery drive, the speed boundary conditions are the same for both compressor and turbine. The thermodynamic properties of the working fluids are computed through an interface between the solver and the NIST Refprop database [25].

The heat exchangers and pipes are modelled as 1D equivalent objects. For the heat exchangers, the geometrical inputs are used to define the properties of the equivalent 1D channels. The performance data, related to several operating conditions of the devices, are provided by the manufacturers for the primary heater and the gas cooler, while for the PCHE recuperator, they have been retrieved through more complex models [26]. These data are then employed to calculate the best fitting coefficients of the Nusselt-Reynolds (Nu-Re) correlations for the equivalent 1D networks that approximate the heat exchangers [4].

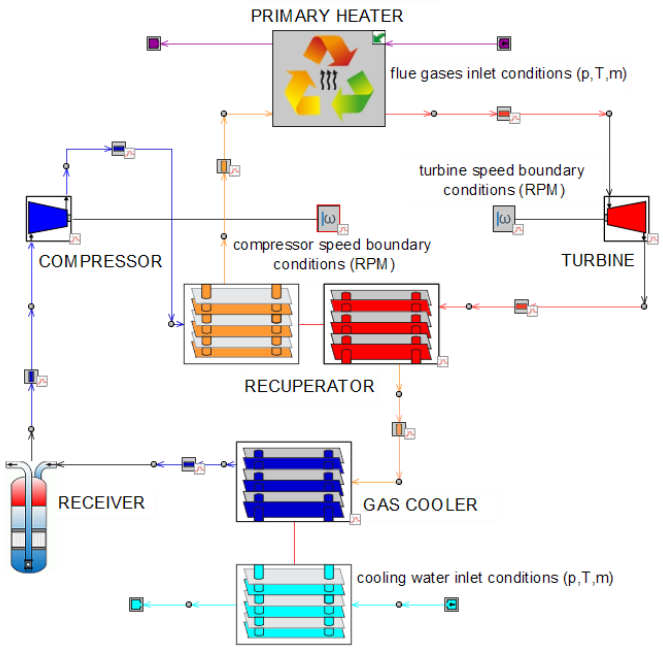

Figure 2: GT-SUITE model of the HT2C test facility.

Table 1: Flow parameters and geometrical features of the heat exchangers embedded in the sCO_2 heat to power conversion unit: primary heat exchanger or heater (PHX), Printed Circuit recuperator (PCHE) and gas cooler (PHE).

Flow parameters (heating/cooling fluid)		PHX	PCHE	PHE
Nominal heat duty	kW	388.3	630.0	237.5
Nominal UA value	kW/K	20.3	20.3	16.8
Pressure drop	kPa	64/11	120/128	8.7/89.1
Geometrical features (heating fluid/cooling fluid)				
Hydraulic diameter	mm	1.9/500	1.22	4.52
Wetted perimeter	mm	5.97	5.12	398.6
Cross sectional area	mm^2	3542/2.5e5	7121	451
Heat transfer area	m^2	14.8	12.0	6.2
Tubes/Channels/Plates	#	1250	2268	84
Material	-	IN-617	SS316L	SS316L
Dry weight	kg	97.6	305.0	52.4

Even though this modelling methodology is common to all the three heat exchangers considered, the gas cooler requires an additional correlation to account for possible condensation of CO_2. In this case, to predict the phase change, the formation of vapor bubbles or liquid droplets is addressed by evaluating the fluid density in each sub volume, while the two-phase area is computed using the vapour Rayleigh-Plesset formulation [27].

The pressure drops are computed using a modified version of the Colebrook relationship [28], which is valid for the turbulent regime (Re_D>2100). Table 1 reports the flow

parameters and the geometrical features of the heat exchangers. A more extensive description of the modelling methodology is available in [4].

Pipes are considered as adiabatic and localized pressure drops are neglected. Only distributed ones are considered. The receiver has been modelled as a container (capacity) with fixed volume. It is situated downstream the gas cooler to absorb the thermal expansion of the fluid in the circuit, decoupling the high from the low-pressure side of the system (Figure 2). Its volume is 0.165 m^3 and accounts for almost 50% of the overall system capacity.

Mechanical and electrical losses of the electric motors and generators for turbomachines as well as the parasitic losses of the system ancillaries (water cooling pump and fans, oil pump for shaft lubrication, CO_2 drainage compressors) have been discarded. As such, all powers reported onwards are thermal.

TURBOMACHINERY INTEGRATION

As in the case of the CGT unit of the HT2C test facility, in the baseline case for this study, compressor and turbine rotate at the same speed. The performance maps of these machines result from 3D RANS CFD simulations whose modelling methodology has been discussed in [29]. The 3D modelling approach has been benchmarked against experimental data available from the Sandia National Laboratories [18]. The actual maps will be validated in the future against the experimental data once the facility will be commissioned. Inlet boundary conditions of the 3D model were the total pressure and temperature as well as the flow direction, which is considered normal to the boundary. Outlet average static pressure has been chosen as outlet boundary condition. The compressor operating and isentropic efficiency maps can be found in Figure 3.

Since the compressor operates close to the critical point, the real gas properties of the fluid must be considered and the use of reduced quantities via normalization can lead to errors in the compressor performance predictions [30]. To overcome this issue, the model considers multiple compressor maps at four reference states that span the whole CO_2 critical region (308.15K at 70, 75, 80 and 85 bar). At least five pressure ratios for each revolution speed are required to ensure an accurate interpolation of the operating curves. Beyond the speed range and the operating range available from the calibration data, a linear extrapolation method is used to predict the performance of the turbomachines. The extrapolated curves are mostly used to ensure a continuity during the starting phase of the numerical simulations. The small distortion located near the surge line at high revolution speeds is due to the supercritical CO_2 thermophysical properties, which affect the pressure changes inside the compressor at different speeds.

The compressor design resulted in the optimal operating region located close to the surge line, as shown in Figure 3.b, where the isentropic efficiency assumes a value of 0.8 in a range of revolution speeds and pressure ratios of 50000-90000 RPM and 1.3-2.0 respectively.

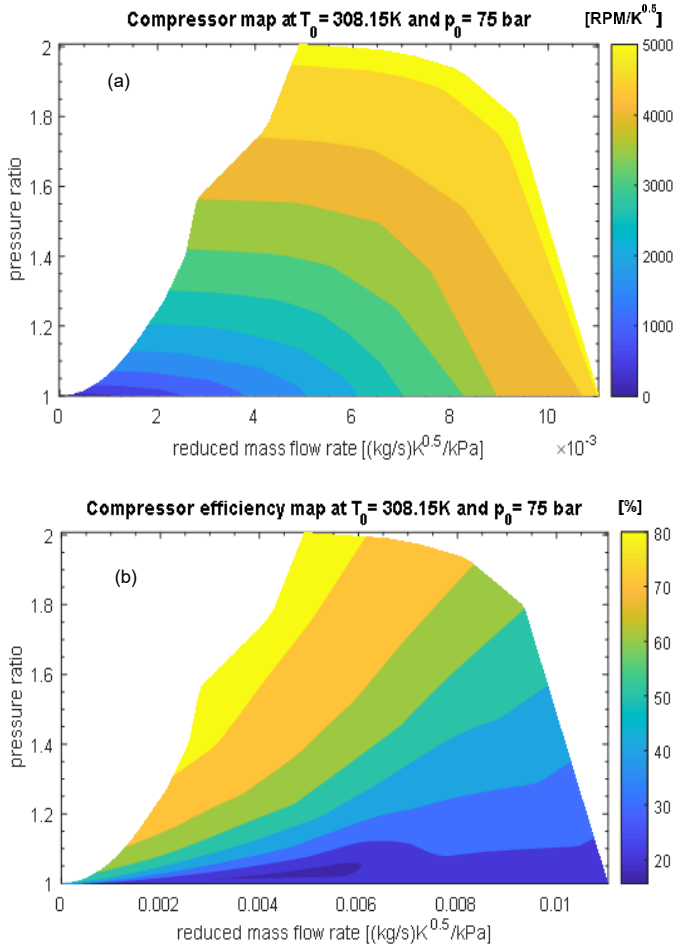

Figure 3: performance (a) and total to static isentropic efficiency maps (b) plotted respect the total to static pressure ratio and to the reduced mass flow rate. Reference state is 308.15K and 75bar. Revolution speed in (a) is expressed in reduced revolutions per minutes [RPM/$K^{0.5}$], efficiency in (b) expressed in percentage points.

The turbine maps are reported in Figure 4 and are represented in a typical format adopted in turbomachinery [31]: the operating curves (Figure 4.a) and the total-to-static isentropic efficiency (Figure 4.b), expressed in percentage units, are reported as a function of the pressure ratio, the reduced mass flow rate [(kg/s)$K^{0.5}$/kPa] and the reduced revolution speed [RPM/$K^{0.5}$]. The reference state is 650K and 145 bar.

To assess the advantages of having independent turbomachinery drives, a new turbine has been designed following the methodology developed in [22]. The approach considers a three-step technique to design and optimise the turbine performance in part load/off-design conditions. A mean line procedure considers the design of the rotor, the stator and the volute of the turbine, assumed for simplicity as a circular cross section, in order to accurately estimate the fluid dynamic losses.

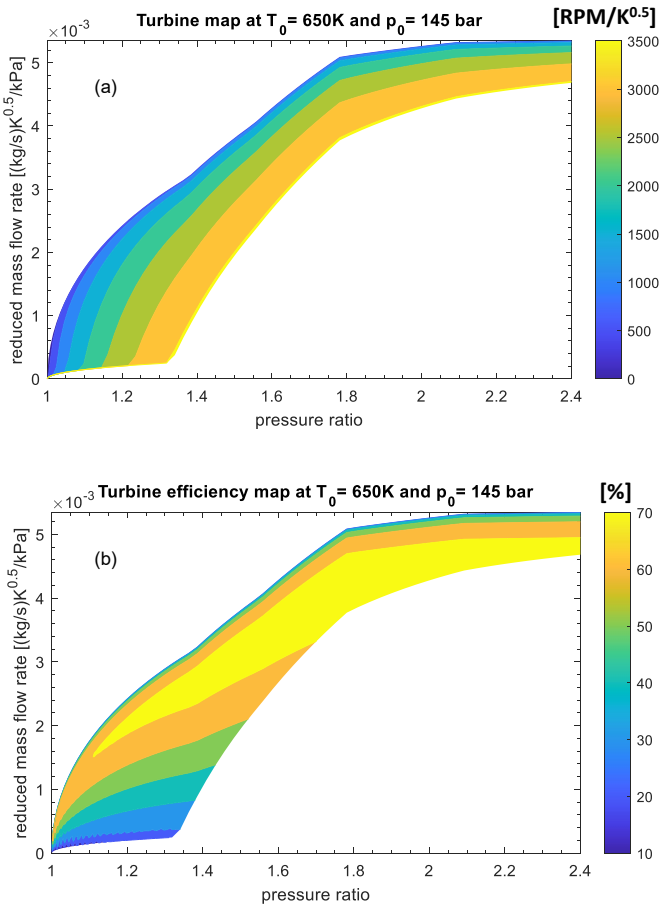

Figure 4: Turbine performance (a) and total to static isentropic efficiency maps (b) for Coupled Drive (CD) case plotted respect the reduced mass flow rate and the total to static pressure ratio. Reference state is 650.00K and 145bar. Revolution speed in (a) is expressed in reduced revolutions per minutes [RPM/$K^{0.5}$], efficiency in (b) expressed in percentage points.

To start the procedure, first, a set of geometrical and thermodynamics parameters are required [32, 33], chosen respectively by manufacturability considerations and according to the design operating point of the sCO_2 system object of this work.

Given these input data, an isentropic efficiency value at the design point of the turbine is estimated, which is used to compute the enthalpy drops in the rotor, stator and in the volute.

Consequently, a new isentropic efficiency value is calculated and compared with the previous estimated one. The procedure is repeated iteratively until a convergence is achieved. The MATLAB optimisation toolbox has been used to optimise the inlet parameters, using as objective function the isentropic efficiency of the machine. The resulting optimized numbers for key main dimensions including loading coefficient (φ), flow coefficient (ψ), rotor blade (Z) etc. were transferred to RITAL.

After this preliminary design stage, RITAL, a commercial 0D/1D software tool [34], has been used to calculate the turbine performance at off-design conditions, and thus obtain the operating and isentropic efficiency map of the machine. To do so, RITAL has been firstly calibrated to predict the turbine design conditions and then to calculate the off-design performance of the expander. The calibrated parameters of turbine design are presented in Table 2.

Table 2. Turbine design parameters for Coupled (CD) and Independent drive (ID) solutions

Design parameters		**CD**	**ID**
Inlet Pressure	[bar]	127.5	127.5
Inlet Temperature	[K]	653.15	753.15
Mass flow rate	[kg/s]	2.25	2.25
Pressure Ratio	[-]	1.7	1.7
Performance parameters			
Loading coefficient	[-]	0.854	0.918
Flow coefficient	[-]	0.090	0.215
Isentropic efficiency	[-]	0.75	0.75
Power output	[kW]	110	122.8
Geometrical features			
Wheel diameter	[mm]	57.1	50.9
Axial length	[mm]	15	15
Stator blades	#	6	17
Rotor blades	#	6	14

The maps resulted from this design and optimization process have been implemented in GT-SUITE™ are displayed in Figure 5. The discontinuity in the turbine maps noticeable is due to the extrapolation of the turbine operating curves and isentropic efficiency lines made by the software for pressure ratios lower than 1.4.

Compared to the speed constrained turbine design, the independent one can provide a higher range of CO_2 mass flow rates even at lower pressure ratios. For instance, with reference to a pressure ratio of 1.2, the new turbine design can process for its entire revolution speed range a mass flow rate of working fluid going from 1.59 kg/s to 2.51 kg/s. For the same pressure ratio, the old turbine design could process a CO_2 mass flow rate varying in range only from 0.11 kg/s to 1.48 kg/s respectively. As concerns the isentropic efficiency, the old design presents an optimal operating value in a wider range of mass flow rates and pressure ratios compared to the new one.

RESULTS AND DISCUSSION

To investigate the benefits deriving from the adoption of independently driven turbomachinery, a series of simulations at different operating conditions of the sCO_2 heat to power conversion system have been carried out varying the thermal load supplied by the waste heat source. In particular, since the heat load of this stream is completely defined by its mass flow rate and inlet temperature, these conditions were changed during the simulations with respect to the design point at 1 kg/s and 923.15K. On the other hand, the cooling water mass flow rate

and inlet temperature have been kept equal to 1.6 kg/s and 298.15K respectively.
In each case, the net power output has been maximised acting on the compressor and turbine revolution speeds as independent variables. The optimisation algorithm employed is the Nelder Mead SIMPLEX one, which is suitable for finding a local minimum and at a low computational cost since no calculations of derivative terms are involved. For the independent drive configuration, two independent variables must be optimised, the compressor and turbine revolution speeds, and thus the method is a pattern search that compares function values at the three vertices of a triangle.

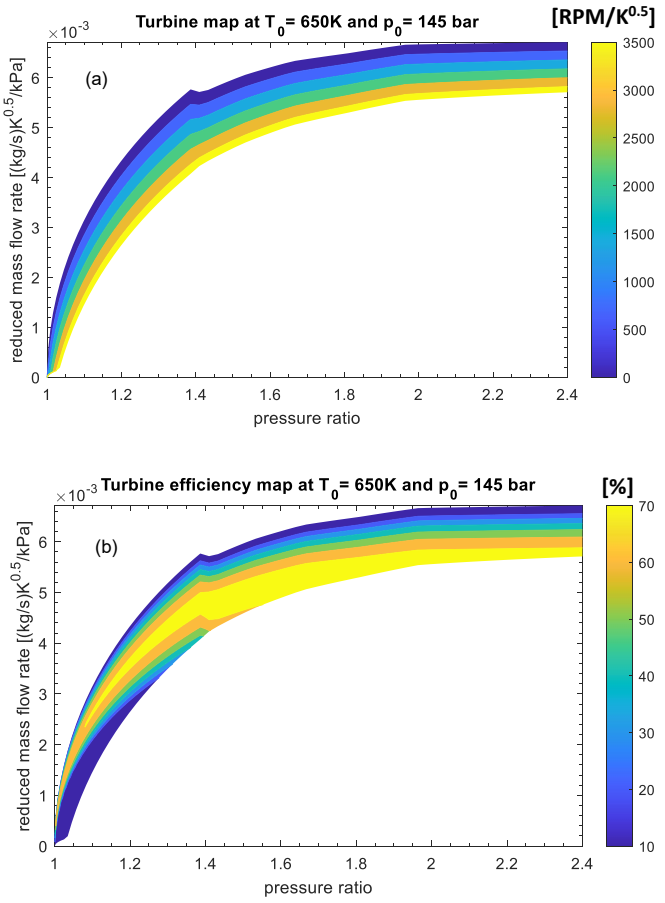

Figure 5: Turbine performance (a) and total to static isentropic efficiency maps (b) for Independent Drive (ID) case plotted respect the reduced mass flow rate and the total to static pressure ratio. Reference state is 650.00K and 145bar. Revolution speed in (a) is expressed in reduced revolutions per minutes [RPM/$K^{0.5}$], efficiency in (b) expressed in percentage points.

The worst vertex, is rejected and replaced with a new vertex. A new triangle is formed and the search is continued. The process generates a sequence of triangles for which the values of the optimization function at the vertices get smaller and smaller. The size of the triangles is reduced and the coordinates of the minimum point are found. When the sCO_2 system configuration with coupled turbomachines is considered, the optimisation method is similar but considers a segment line instead of a triangle, since only one independent variable must be optimised. Even if the algorithm adopted also allows to perform constrained optimisations by penalizing the regions which violate the constraints imposed [24, 35], in this study, no constraints have been imposed.

The results of the optimisation for the Coupled Drive (CD) case have been reported in Figure 6. For reduced thermal loads, i.e. waste heat mass flow rate and inlet temperature below 0.7 kg/s and 773K respectively, the system is not able to generate any power output since the power required by the compressor is equal or greater than the one generated by the fluid expansion in the turbine. This is mainly due to the low design pressure ratio of the cycle, which together with the low divergence of the CO_2 isobaric lines, requires the achievement of high turbine inlet temperatures to reach a positive power output. At higher thermal loads, i.e. for waste heat source mass flow rates and inlet temperatures above 1.3 kg/s and 1073K respectively, the sCO_2 unit is able to generate a maximum power output of 105kW, thanks to an increased turbine inlet temperature and cycle pressure ratio which consequently lead to a higher cycle thermal efficiency and enthalpy drop across the turbine.

Figure 7 shows the net power difference between independent and coupled turbomachinery drive simulations (ID-CD). At the same operating conditions, the adoption of independent drives for the turbine and compressor can lead to an improvement of the system performance. Indeed, for a heat source inlet temperature of 973 K and mass flow rates higher than 1.0 kg/s, 1.1 kg/s and 1.2 kg/s, decoupling the turbomachines leads to a net power output increase of 10 kW, 20 kW and 30 kW respectively. Close to the design point (1 kg/s, 923.15K), the independent speed regulation does not lead to any performance benefits. When the heat source mass flow rate and inlet temperature are below 1 kg/s and 900K, there is actually a slight decrease of the system net power output up to -10 kW. Hence, the independent drive solution is only beneficial for part-load operating conditions exceeding the design point. In particular, the additional power output is more affected by the heat source temperature than the mass flow rate.

A deeper insight on the power output trends is provided by the optimised performance of the compressor and the turbine in both the configurations investigated. In particular, Figure 8 displays the power required by the compressor (Figure 8.a) and the one generated by the turbine (Figure 8.b) when the machines are coupled. The compressor presents a low sensitivity to the thermal load supplied by the waste source, showing a power consumption increase of the 6.7% for a decrease of the thermal load of 30% (Figure 8.a). This worse performance mainly occurs since a reduction of the heat source inlet temperature or mass flow rate do not allow supercritical conditions of the working fluid at the compressor inlet. For the same thermal load variation,

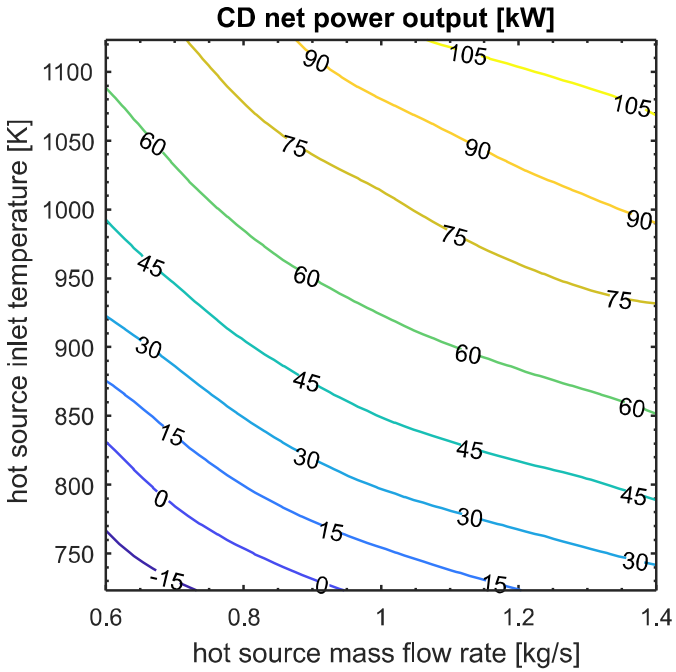

Figure 6: Net thermal power output at different heat inputs to the sCO_2 unit – Coupled turbomachinery Drive (CD)

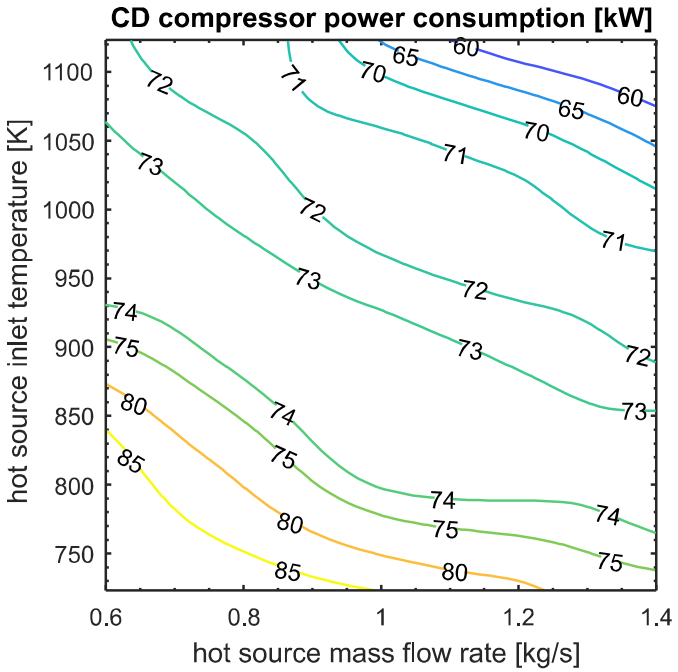

(a)

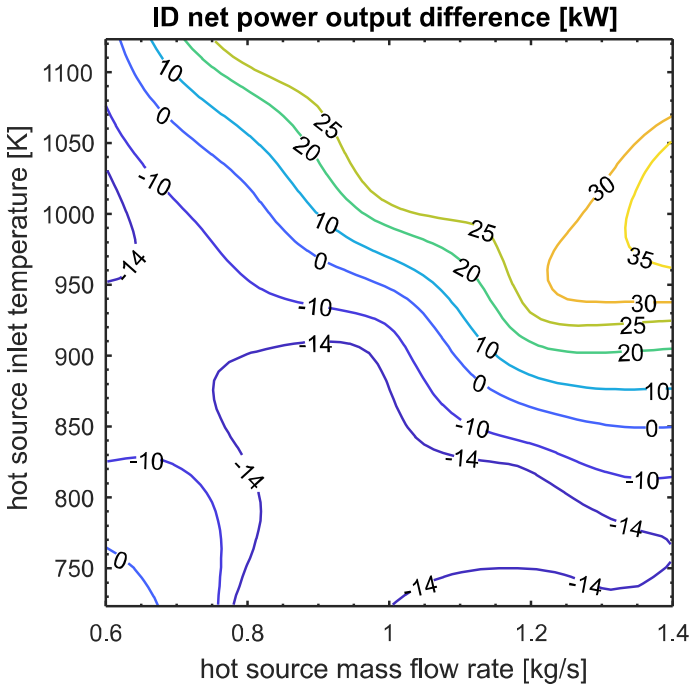

Figure 7: Differential net power output between Independent and Coupled turbomachinery Drive solutions (ID- CD)

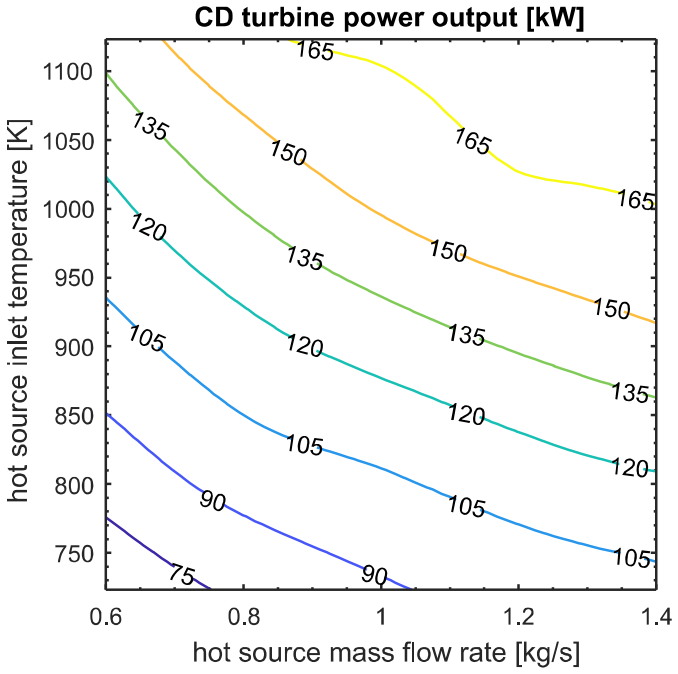

(b)

Figure 8: Compressor (a) and turbine (b) thermal power for coupled drive (CD) configuration

the turbine shows a performance decrease of the 36.4% (Figure 7.b). Therefore, the optimisation of the turbine operating conditions based on the heat source availability is the most effective contribution to improve the system performance.

This is further evidenced in Figure 9, which shows the difference between the optimised compressor power consumption (Figure 9.a) and the power generated by the turbine (Figure 9.b) considering an ID configuration and the ones obtained in CD configuration. In fact, the improvement of sCO_2 system performance achieved in the ID case showed in Figure 7 is driven by an improvement of the turbine performance rather than the compressor ones. For instance, for a waste heat source mass flow rate and inlet temperature of 1 kg/s and 1000K respectively, the 20 kW increase in the system net power output (Figure 7) results from the optimisation of the turbine operating conditions (30 kW increase in the power generated, Figure 9.b). The performance increase is obtained thanks to a higher mass flow rate of CO_2 flowing across the machine which leads however to a small decrease in the compressor performance (10 kW increase in the power consumption, Figure 9.a) since the cycle pressure ratio remains almost constant.

Figure 10 shows the optimal speeds for the independent and coupled turbine designs. With reference to Figure 10.a, the turbine performance optimisation in the ID configuration is achieved by increasing the machine revolution speed accordingly to the thermal load provided by the heat source. In fact, assuming a unitary mass flow rate of the waste heat source, when the inlet temperature of the flue gas increase from 950K up to 1100K, the optimised turbine revolution speed is increased from 86000 RPM to almost 100000 RPM. For the CD configuration the revolution speed range of the turbine is constrained by the compressor design and cannot thus assume values higher than 90000 RPM, as showed in Figure 10.b, which displays the optimal revolution speed assumed by the compressor and the turbine for the different thermodynamic conditions of the waste heat source. Furthermore, it can be noticed in Figure 10 that when the thermal load supplied by the waste heat source decreases (mass flow rate and inlet temperature lower than 1 kg/s and 950K respectively) the maximisation of the system power output is achieved in both cases by lowering the revolution speed of the turbomachines, which are decreased down to the minimum value of 80000 RPM and 82000 RPM for the ID and CD configuration respectively. Indeed, the maximum and minimum value of the pressure in the cycle are fixed by the thermal loads in the primary heater and gas cooler respectively. For this given cycle pressure ratio, a decrease of the machine revolution speed leads to a slight increase of the CO_2 mass flow rate flowing in the sCO_2 loop, which consequently positively impacts the system net power output.

CONCLUSIONS

This paper assessed the performance implications of simple regenerative supercritical CO_2 (sCO_2) power cycles equipped with radial turbomachines being simultaneously or independently driven. The case study analysed was the 50kWe sCO_2 test facility at Brunel University London, whose design conditions include a cycle pressure ratio of 1.7 and a turbine inlet temperature of 673K. The research methodology employed a 3D RANS CFD and a mean line approach for the design of the coupled and independent drive turbine configurations respectively. The turbine maps generated through the aforementioned methods have been used as inputs to a numerical one-dimensional modelling platform whose sub-models have been calibrated against equipment data of the test facility. The performance comparison was carried out at different heat inputs to the sCO_2 loop, which in the current waste heat recovery application came from a flue gas stream of 1kg/s at 923K. Despite being designed for the same nominal performance of 75% total-static isentropic efficiency, the need to match the compressor operating conditions led to very different turbine maps. For instance, at a pressure ratio of 1.2, the independently driven turbine allows a larger operational flow range (1.59-2.51 kg/s) than the speed constrained one (0.11 to 1.48 kg/s). The same design specifics led to similar nominal performance regardless of the turbine employed. For part load conditions below the design point, the independent drive solution leads to worse performance. On the other hand, when the heat source mass flow rate and temperature are above the design point, the dual optimisation of compressor and turbine speeds leads to a net power output increases up to 30%. This is primarily due to a higher mass flow rate in the sCO_2 loop that in the coupled drive configuration would significantly worsen the compressor efficiency. Hence, a coupled turbomachinery drive is advisable should the sCO_2 heat to power block operate close or below design conditions. Instead, an independent drive solution is preferred for frequent part load operation above the design specifics.

Future research will consider the cost and scale aspects for an optimal techno-economic design of simple regenerative sCO_2 power units. Additional focus will be devoted to the aerothermal compressor design optimisation to take into account the operational challenges in the critical region. Another driver of future research will be the scalability considerations for large sCO_2 power applications that will likely employ axial turbomachines rather than radial ones.

ACKNOWLEDGEMENTS

The research presented in this paper received funding from the European Union's Horizon 2020 research and innovation program under grant agreement No. 680599. Aspects of the work are also funded by the Engineering and Physical Sciences Research Council (EPSRC) of the UK under research grants (i) EP/V001752/1 'Industrial waste heat recovery using supercritical carbon dioxide cycles (SCOTWOHR)'; (ii) EP/P004636/1 'Optimising Energy Management in Industry (OPTEMIN)'; (iii) EP/K011820/1 related to the Centre for Sustainable Energy Use in Food Chains (CSEF), an End Use Energy Demand Centre funded by the Research Councils UK.

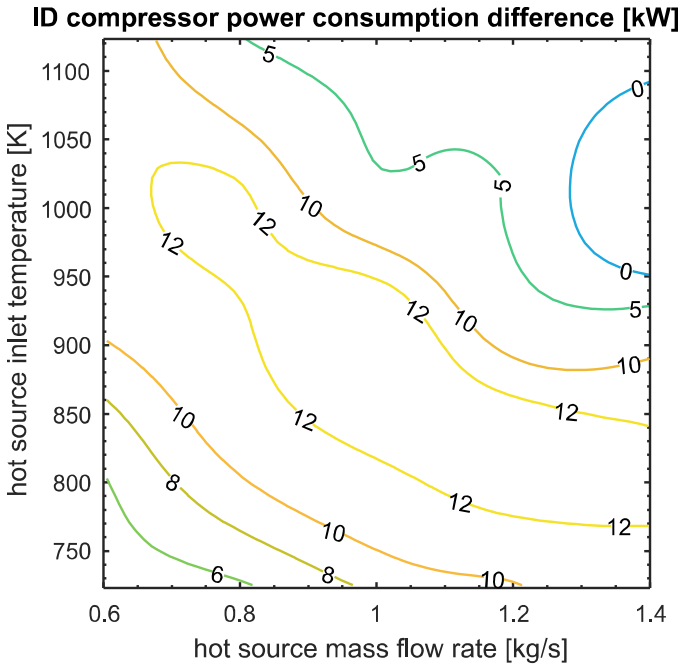

(a)

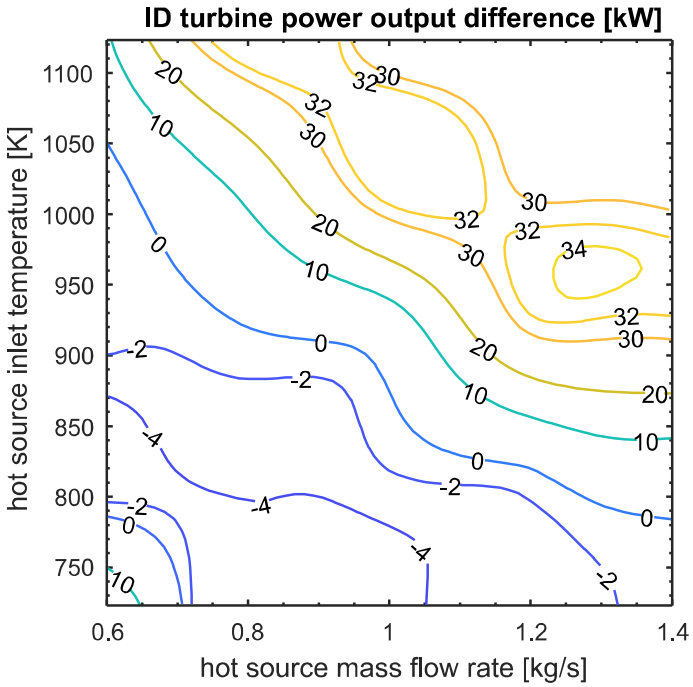

(b)

Figure 9: Compression (a) and expansion (b) powers difference between the independent and coupled drive solutions (ID-CD)

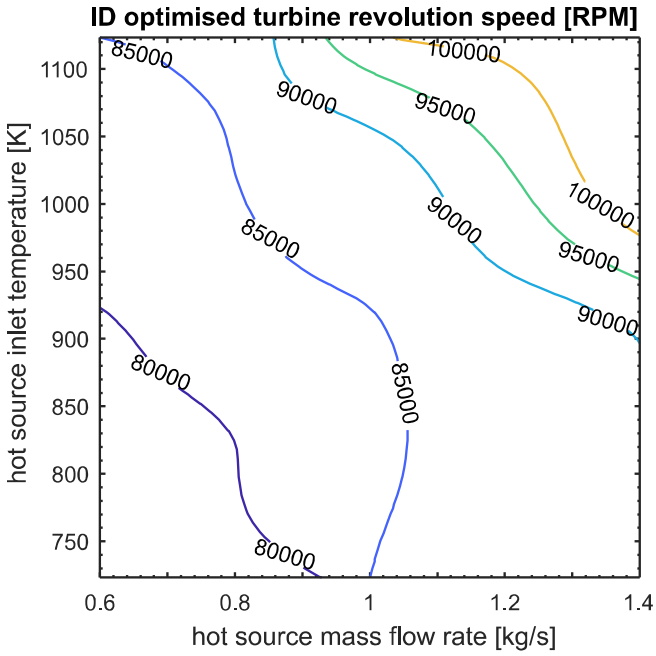

(a)

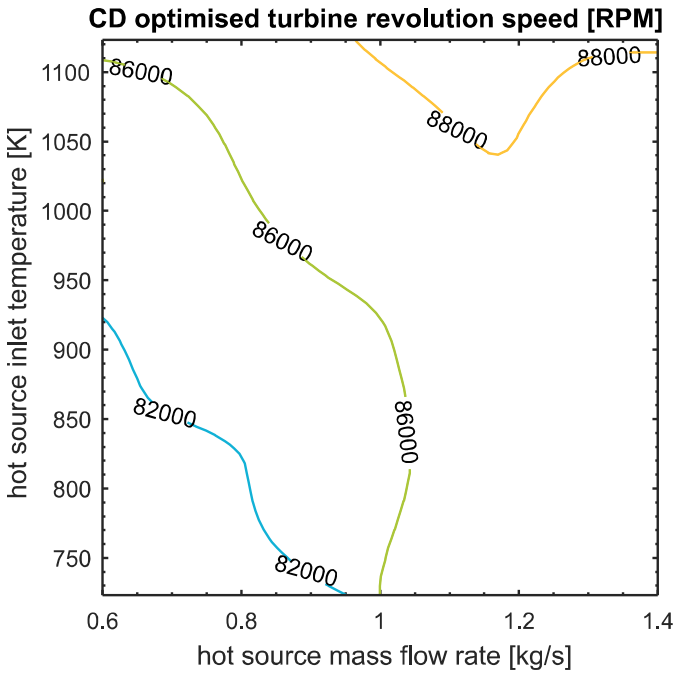

(b)

Figure 10: Optimised speeds for the Independent (a) and Coupled (b) turbine design configurations

REFERENCES

[1] M. White et al., Review of supercritical CO2 technologies and systems for power generation, Applied Thermal Engineering, 2021, DOI: 10.1016/j.applthermaleng.2020.116447.

[2] K. Brun, P. Friedman, R. Dennis, Fundamentals and Applications of Supercritical Carbon Dioxide (sCO2) Based Power Cycles, 2017, ISBN 978-0-08-100804-1.

[3] M. Mecheri, Y. L. Moullec, Supercritical CO2 Brayton cycles for coal-fired power plants, Energy, 2016, DOI: 10.1016/j.energy.2016.02.111.

[4] M. Marchionni, G. Bianchi, S. A. Tassou, Transient analysis and control of a heat to power conversion unit based on a simple regenerative supercritical CO2 Joule-Brayton cycle, Applied Thermal Engineering, 2021 DOI: 10.1016/j.applthermaleng.2020.116214.

[5] S. Bedogni, D1.2 – Report on Flexibility constraints, Load scenarios definition, 2018, URL: www.sCO2-flex.eu/documents/

[6] Echogen power systems, URL: www.echogen.com/.

[7] J. Marion et al., The STEP 10 MWe sCO2 pilot plant demonstration, in: Proceedings of the ASME Turbo Expo 2019. DOI: 10.1115/GT2019-91917.

[8] D. Freed et al., Progress update on the Allam cycle: Commercialization of Net Power and the Net Power demonstration facility, in: 14th Greenhouse Gas Control Technologies Conference Melbourne, 2018.

[9] 8 Rivers Capital, Allam cycle zero emission coal power plant, DOE Grant Proposal 89243319CFE000015, 2019.

[10] F. Crespi et al., Supercritical carbon dioxide cycles for power generation: A review, Applied Energy (2017), DOI: 10.1016/j.apenergy.2017.02.048.

[11] M. Marchionni et al., Techno-economic assessment of Joule-Brayton cycle architectures for heat to power conversion from high-grade heat sources using CO2 in the supercritical state, Energy, 2018, DOI: 10.1016/j.energy.2018.02.005.

[12] Y. Ahn et al., Review of supercritical CO2 power cycle technology and current status of research and development, Nuclear Engineering and Technology, 2015, DOI: 10.1016/j.net.2015.06.009.

[13] R. Fuller et al., Turbomachinery for supercritical CO2 power cycles, ASME Turbo Expo, 2012, DOI: 10.1115/GT2012-68735.

[14] A. J. Hacks et al., Operational experiences and design of the sCO2-HERO loop, in: 3rd European Supercritical CO2 Conference, 2019, DOI:10.17185/duepublico/48906.

[15] E. M. Clementoni et al., Startup and operation of a supercritical carbon dioxide Brayton cycle, Journal of Engineering for Gas Turbines and Power, 2014, DOI:10.1115/1.4026539

[16] G. Bianchi et al., Design of a high-temperature heat to power conversion facility for testing supercritical CO2 equipment and packaged power units, Energy Procedia, 2019, DOI: 10.1016/j.egypro.2019.02.109.

[17] M. Marchionni et al., Review of supercritical carbon dioxide (sCO2) technologies for high-grade waste heat to power conversion, SN Applied Sciences, 2020, DOI: 10.1007/s42452-020-2116-6.

[18] S. A. Wright et al., Operation and analysis of a supercritical CO2 Brayton cycle, 2010, DOI: 10.2172/984129.

[19] M. Marchionni et al., An appraisal of proportional integral control strategies for small scale waste heat to power conversion units based on organic Rankine cycle, Energy, 2018, DOI: 10.1016/j.energy.2018.08.156.

[20] J. J. Dyreby et al., Design and Part-Load Performance of Supercritical Carbon Dioxide Power Cycles, 2013, DOI: 10.1115/GT2013-95824.

[21] D. Alfani et al., Part-load operation of coal fired sCO2 power plants. in: 3rd European Conference on Supercritical CO2 (sCO2) Power Systems, 2019. DOI: 10.17185/duepublico/48897.

[22] F. Alshammari et al., Off-design performance prediction of radial turbines operating with ideal and real working fluids. Energy Conversion and Management, 2018, DOI: 10.1016/j.enconman.2018.06.093.

[23] M. De Miol et al., Design of a single-shaft compressor, generator, turbine for small-scale supercritical CO2 systems for waste heat to power conversion applications. 2nd European sCO2 Conference 2018. DOI:10.17185/duepublico/46086

[24] Gamma Tech., GT-SUITE Flow Theory Manual, 2020.

[25] E. Lemmon et al., NIST Standard Reference Database 23: Reference Fluid Thermodynamic and Transport Properties-REFPROP, National Institute of Standards and Technology, Standard Reference Data Program, Gaithersburg, 2018.

[26] M. Marchionni et al., Numerical modelling and transient analysis of a printed circuit heat exchanger used as recuperator for supercritical CO2 heat to power conversion systems, App Ther Eng, 2019, DOI:10.1016/j.applthermaleng.2019.114190.

[27] A. Prosperetti, A generalization of the Rayleigh–Plesset equation of bubble dynamics. Phys Fluids 1982;25:409. DOI:10.1063/1.863775.

[28] D. Brkić, Review of explicit approximations to the Colebrook relation for flow friction. J Pet Sci Eng 2011;77:34–48. DOI:10.1016/J.PETROL.2011.02.006.

[29] S.S. Saravi, S.A. Tassou, An investigation into sCO2 compressor performance prediction in the supercritical region for power systems, Energy Procedia, 2019, DOI:10.1016/J.EGYPRO.2019.02.098.

[30] M. White, AI Sayma. A preliminary comparison of different turbine architectures for a 100 kW supercritical CO2 Rankine cycle turbine 2018.

[31] S. Son et al., Development of supercritical CO2 turbomachinery off-design model using 1D mean-line method and Deep Neural Network. Applied Energy, 2020. DOI: 10.1016/j.apenergy.2020.114645.

[32] H. Moustapha et al., Axial and radial turbines. Conceptsnrec Com 2003:10.

[33] RH. Aungier, Turbine Aerodynamics: Axial-Flow and Radial-Flow Turbine Design and Analysis. ASME Press; 2006. doi:10.1115/1.802418.

[34] NREC. RITAL | Preliminary Design n.d. https://www.conceptsnrec.com/solutions/software/computer-aided-engineering/preliminary-design/rital.

[35] J. A. Nelder, R.Mead, A simplex method for function minimization. The computer journal, 1965, 7(4), 308-313.

DOI: 10.17185/duepublico/73949
URN: urn:nbn:de:hbz:464-20210330-094323-9